Identification of non-linear closed loop systems

Koene, K.J.A.

Award date:
2003

Eindhoven University of Technology
Department of Electrical Engineering
Control Systems

Identification of Non-linear closed Loop Systems

by

K.J.A. Koene

Master of Science thesis

Project period: February 2003 – November 2003
Report Number: 03A/10

Supervisors:
Prof. dr. ir. P.P.J. van den Bosch

Additional Commission members:
Dr. ir. N.A.W. v. Riel
Dr. H.H.M. Korsten

Identification of Non-Linear Closed Loop Systems

Analysis of the Human Respiratory System in Hyperoxia

K.J.A. Koene

Department of Electrical Engineering, Eindhoven University of Technology

Abstract

A model of the human respiratory system is implemented and used for parameter estimation. The presented model includes the gas exchange dynamics ('plant') and respiratory controller, which are both based on models found in literature. One of the improvements to the plant-model is that for the oxygen dissociation curve, a lookup-table is used instead of a mathematical expression. This increases the accuracy of the implemented curve, under the assumptions made. One of the general problems in identifying the respiratory system is that it operates in closed loop under normal circumstances. To circumvent some of the problems associated with closed loop identification, rebreathing tests are used to acquire the ventilatory data for parameter estimation. Another difficulty in identification is that the presented model contains several non-linearities in both plant and controller, which have an effect on the uncertainty of the estimations. By using a novel Monte Carlo approach to approximate the joint confidence regions of the estimates, the effect of non-linearities is accounted for. In this study, the focus of the identification is the respiratory controller in hyperoxia. The choice for the parameters to be estimated is made by studying the parameter dependencies that exist in the used three-output (frequency, tidal volume and total ventilation) controller model. Two different approaches to estimation are taken. In the first approach the measured total ventilation is fit to the respective controller output, and the second approach seperately fits breathing frequency and tidal volume. Because of the large intra-subject variation of breathing pattern, the second approach does not always result in a good fit of frequency and/or tidal volume. The first approach on the other hand, produces acceptable results in almost all cases. Generally speaking, fitting the total ventilation produces more reliable estimates and better fits than fitting both frequency and tidal volume. Thus, based on the responses for hyperoxic rebreathing, it seems more useful to base a general model of the respiratory controller on the total ventilation, than on frequency and tidal volume separately.

Introduction

Mathematical modelling of the respiratory system is a field of research that was pioneered in the mid-1950s by Grodins et al, eventually leading to one of the first models of the respiratory system [4]. Since then, all sorts of advances have been made in understanding the complicated workings of the human respiration. This led to many different respiratory models, some focussing on particular (isolated) aspects of the system [10], and some focussing on the system as a whole [2], [17].

One of the difficulties in modelling the human respiration is that under normal operating circumstances the respiratory system functions in closed loop. Furthermore, it contains several non-linearities, e.g. the dissociation curves of CO_2 and O_2, which relate partial pressure to content.

In this study, a model of the respiratory system is presented, including the gas exchange dynamics, respiratory controller and relatively simple, but effective descriptions of the dissociation curves. This model does not strive to explain and/or simulate clinical/pathological problems. Instead the emphasis will be on structured identification and estimation of the controller parameters.

Model Formulation

The respiratory model consists of two separate parts: the gas exchange dynamics (hereafter addressed as the 'plant'), which describe the transport and use/production of the respiratory gases in the body, and the respiratory controller, which regulates the ventilation based on the concentrations of O_2 and CO_2 in the body. A functional block diagram of the respiratory system is shown in figure 1.

Gas Exchange in Lungs and Tissue

The model for the gas exchange used in this study is an adaptation from the model derived by Chiari et al [2]. This model comprises three compartments

(lungs, tissue and brain), including transport delays and shunted blood. In figure 2, a schematic representation of the plant can be found, including the different compartments. The assumptions made for this model are stated in Appendix A. In Appendix B, the nominal values of the parameters, as well as the steady-state values can be found.

The lung is described by a single compartment, which is ventilated by a continuous unidirectional stream of gas. Explicitly including the pulmonary shunt, the mass balance for O_2 and CO_2 leads to the following equation for the alveolar partial pressure:

$$V_A \cdot \frac{dP_A}{dt} = Vdot \cdot (P_I - P_A) + \lambda \cdot Q \cdot (1-s) \cdot (C_v - C_e)$$

Where V_A is the equivalent alveolar volume (l), Vdot is the alveolar ventilation (l/min), P_A and P_I are the alveolar and inspiratory partial pressures (mmHg), λ is the conversion-factor for Standard Temperature and Pressure Dry-units (STPD) to Body Temperature and Pressure Saturated-units (BTPS), Q is the cardiac output (l/min), s is the shunted fraction of blood, and C_v and C_e are the mixed venous and end-cappilary concentrations (l/l). The alveolar and end-capillary pressures are assumed to be equal.

Because of the shunted blood (the blood that does not take part in gas exchange), the alveolar partial pressure P_A does not equal the arterial partial pressure P_a. Instead, the arterial concentration is given by the following equation:

$$C_a = (1-s) \cdot C_e + s \cdot C_v$$

The subscripts *a*, *e* and *v* denote the arterial, end-capillary and venous concentrations respectively.

In the model, all tissue is lumped in a single compartment. The mass balance in the tissue compartment is as follows:

$$V_T \cdot \frac{dC_T}{dt} = Q_T \cdot (C_a - C_{vT}) + M_T$$

In this equation, subscript T indicates the tissue compartment, so that V_T is the equivalent tissue volume (l), C_T is the concentration of gas in the tissues (l/l), Q_T is the tissue blood flow (l/min), C_{vT} is the concentration in the blood leaving the tissue compartment (l/l) and M_T is the gas production rate in the tissue (l/min). This rate is positive for CO_2 (since it is produced) and negative for O_2 (since it is consumed). Different from the model described by Chiari et al, in the presented model the total oxygen consumption rate M (l/min) is defined as follows:

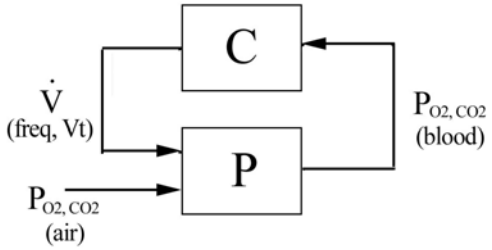

Fig. 1. Functional block diagram of the human respiratory system with controller C and plant P.

$$M_{O2} = Q \cdot \theta$$

Where θ is the amount of used O_2 (in litre) per litre blood. The rate of CO_2 production can be computed from this value by using the respiratory quotient RQ:

$$M_{CO2} = RQ \cdot M_{O2}$$

Identical to the tissue compartment, the mass balance for the brain compartment is:

$$V_B \cdot \frac{dC_B}{dt} = Q_B \cdot (C_a - C_{vB}) + M_B$$

With subscript B denoting the brain-compartment. The gas content of the mixed venous blood can be expressed in terms of C_{vT} and C_{vB} by use of the following equation:

$$C_v = \frac{Q_B}{Q} \cdot C_{vB} + \frac{Q_T}{Q} \cdot C_{vT} = (1-z) \cdot C_{vB} + z \cdot C_{vT}$$

In which z is the fraction of Q entering the tissue compartment.

The need for a separate brain compartment arises from the fact that the CO_2-pressure in the brain (medulla) is an input of the used respiratory controller. The medullary CO_2-pressure (P_m) can be derived from the partial CO_2-pressure in the cerebrospinal fluid (P_{csf}). Assuming that CO_2 diffuses from brain tissue to cerebrospinal fluid (csf) with a speed proportional to the pressure gradient, the P_{csf} can be described by:

$$\frac{dP_{csf}}{dt} = \frac{1}{\tau_B} \cdot (P_B - P_{csf})$$

With τ_B the brain to csf diffusion time constant (min). Finally, the relationship between CO_2-pressure in medulla and csf is:

$$P_m = P_B + (P_{csf} - P_B) \cdot \exp(-k_{cr} \sqrt{Q_B})$$

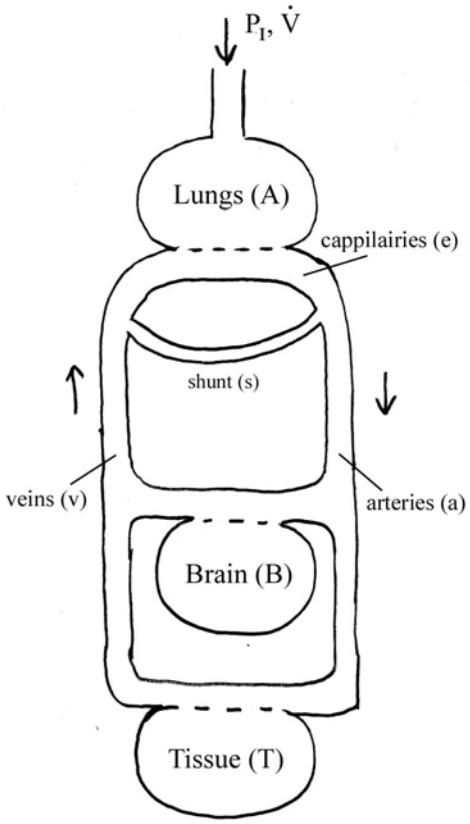

Fig. 2. Global structure of the respiratory plant.

Where k_{cr} ($min^{1/2}/litre^{1/2}$) is a constant characterising the central chemoreceptors.

Dissociation Curves

To solve the equations described above, it is necessary to know the relationship between partial gas pressure in the blood and the corresponding concentration. For CO_2, this relationship is often assumed linear, which is correct in case of a normal working range. In the model, the linear approximation of the CO_2-curve as described by Kelman [3] is used, which accounts for temperature, plasma pH and hematocrit. By assuming constant values for these variables, the elaborate equations of Kelman can be reduced to the following simplified form:

$$C_{CO2} = P_{CO2} \cdot (a + b \cdot S_{O2})$$

Where the values for *a* and *b* are dependent on temperature, plasma pH and hematocrit. Temperature and hematocrit are assumed to be of nominal value. To account for the effect of pH, two different dissociation curves are used: one for the arterial blood (pH = 7.4) and one for the venous blood (pH = 7.36). The fact that the oxygen-saturation (S_{O2}) has a (small) influence on the amount of carbon dioxide in the blood is known as the Haldane-effect.

The O_2 dissociation curve is S-shaped, with a possible shift to the left or right. Factors that cause this shift include the temperature, the blood pH, the concentration of 2,3-diphosphoglycerate (2,3-DPG) and the partial pressure of CO_2 [6]. It can be shown that under normal resting circumstances the influence of temperature, pH and 2,3-DPG is small. More important is the effect of CO_2 on the shift of the O_2-curve (increase in CO_2-concentration means a shift to right, decrease a shift to left), also known as the Bohr-effect. This effect plays an important part in the oxygen transport of the body, so it will be accounted for in the model.

The usual approach to describing the dissociation curve of O_2 is to derive a mathematical expression that approaches a certain reference-curve consisting of measured standard values (e.g. those reported by Severinghaus [13], [14]). Such an expression must meet several requirements: it must be invertible, since the inversed curve is also used in the model, and the expression and its inverse must give a sufficiently accurate description of the reference curve. However, the expressions found in literature (e.g. those by Kelman [8], Sharan et al [15]) fail to meet at least one of these requirements: the accurate equations are not invertible (e.g. [8], [16]), while the invertible ones are not accurate enough (e.g. [15]).

The approach taken in this study is to use a lookup-table containing the reference-data. This way both the requirements for accuracy and invertibility can be met. To account for the Bohr-effect, the partial O_2-pressure is first converted to a 'virtual O_2-pressure', by using the following relationship [2]:

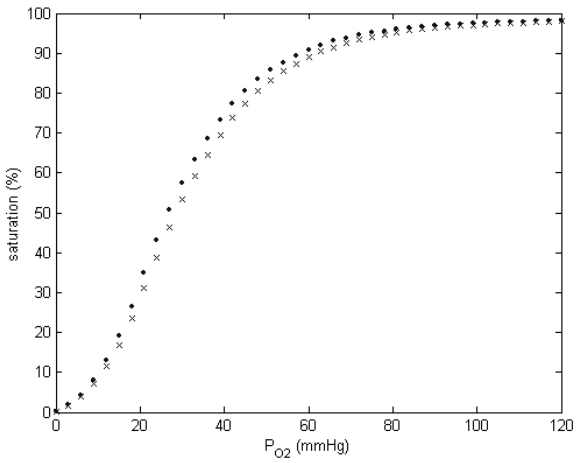

Fig. 3. Oxygen saturation curve including Bohr-effect (x: P_{CO2} = 50mmHg, o: P_{CO2} = 40mmHg).

$$P_{O2vir} = P_{O2} \cdot (\frac{40}{P_{CO2}})^{0.3}$$

After this conversion, the O_2-concentration corresponding to this virtual pressure is found in the table. It is assumed that all of the oxygen in the blood is bound to hemoglobin, i.e. the O_2 solved in the blood plasma is ignored. The implemented curve is pictured in figure 3.

Respiratory Controller

The controller used in the model is the one described by Duffin et al [3]. This controller has the form of the Oxford model, which means that the drive for ventilation is the sum of three components: central and peripheral chemoreflex drives and a basal drive (or wakefulness-drive [10]). The central drive is dependent on P_{CO2}, the peripheral drive on both P_{CO2} and P_{O2}, while the basal drive is independent of the partial pressures. The model features linear relations between ventilation and the partial pressure of carbon dioxide in the blood/brain (above a threshold). Further assumptions with regard to the controller and the nominal values of the controller parameters can be found in Appendices A and B respectively.

In the controller model, the central drive D_c (l) and peripheral drive D_p (l) are described by the following equations:

$$D_c = SD_c \cdot (P_{mCO2} - T_c)$$
$$D_p = \frac{K}{P_{aO2} - AP_{O2}} \cdot (P_{aCO2} - T_c)$$

Where SD_c is the central chemoreflex slope (l/mmHg), T_c is the chemoreceptor threshold (mmHg), K is the slope area constant (l/mmHg) and AP_{O2} is the P_{O2} asymptote (mmHg). These drives add to produce the total drive D (l):

$$D = D_p + D_c$$

Furthermore, there are two thresholds: the chemoreflex drive threshold T_D (l) and the patterning threshold T_P (l), with $T_P > T_D$. When the total drive is smaller than T_D, there is only basal ventilation. For $T_D < D < T_P$ the ventilation Vdot (l BTPS/min), tidal volume V_T (l BTPS) and breathing frequency f (breaths/min) equal:

$$Vdot = S1Vdot \cdot (D - T_D) + Vdot_b$$
$$V_T = S1V \cdot (D - T_D) + V_b$$
$$f = S1F \cdot (D - T_D) + f_b$$

With S1Vdot, S1V and S1F the slopes of ventilation, tidal volume and frequency respectively. When the total drive rises above the patterning threshold, the pattern of breathing changes, corresponding to the changes observed in the respiration of the majority of people. Below T_P, a rise in total ventilation is mainly caused by an increase in tidal volume while above T_P, the rise in ventilation follows largely from an increase in breathing frequency. In other words, the slope of the equations for tidal volume and frequency change, leading to:

$$Vdot = S1Vdot \cdot (T_P - T_D) + S2Vdot \cdot (D - T_P) + Vdot_b$$
$$V_T = S1V \cdot (T_P - T_D) + S2V \cdot (D - T_P) + V_b$$
$$f = S1F \cdot (T_P - T_D) + S2F \cdot (D - T_P) + f_b$$

With this model structure, two different approaches to the parameter estimation can be taken. The first is to simply take the Vdot output, and fit it to measured ventilation data by tuning the respective parameters. This will be called “approach A”. When using this approach, the dead space is accounted for by subtracting the dead space ventilation $Vdot_D$ (in l BTPS/min) from the total ventilation to get the alveolar ventilation:

$$Vdot_A = Vdot - Vdot_D$$

The second proposed approach, called “approach B”, is to fit both frequency and tidal volume to the respective model outputs. When using the V_T and f outputs, the alveolar ventilation is computed by multiplying tidal volume V_T minus dead space volume V_D (l BTPS) with the frequency f. The resulting alveolar ventilation functions as the input of the plant. Thus:

$$\dot{V}_A = f(V_T - V_D)$$

It is expected that the second approach allows for the estimation of more parameters, since more data is available.

Parameter Estimation

After implementing the described respiratory model in Simulink, the focus is on estimating the controller parameters from measurements. In both approaches described above, it will be assumed that the central drive is the only drive to breathe. This is true in a situation of abundant O_2 (‘hyperoxia’). The reason for this assumption is that by evaluating only the central chemoreflex response, the amount of parameters is reduced, which significantly simplifies the parameter estimation procedure. For both approaches, the estimation procedure uses the measured end-tidal P_{CO2} (which is assumed to equal the capillary P_{CO2}) as the input, and then tries to fit the resulting model output – Vdot for approach A, V_T and f for

approach B – to the measured data by tuning the parameters.

Fitting the data is done by means of an optimisation algorithm, which tries to find the minimum of a certain cost function. It is important that a good cost function is used. Also important is the choice of the input signal, since this is one of the factors that can influence the outcome of the estimation procedure.

As can be seen in the previous description of the controller, there are many different parameters. Of course, not all of these variables can be estimated. A choice of the parameters to be estimated can be made by studying the controller equations.

Input Signals

Due to the physiological nature of the respiratory system, the possible input signals are severely limited. Commonly used are pseudo random binary signals (PRBS) on the inspired CO_2 [5] and rebreathing tests [3], tests in which the subject inhales its own exhaled gases by breathing in and out of a bag.

One of the difficulties in identification of the human respiratory system is that normally the system functions in closed loop. General problems with closed loop identification are the effect of feedback noise, as well as the fact that closed loop data typically contains less information about the open loop system. After all, an important purpose of feedback is to make the closed loop system less sensitive to changes. In the case of the respiratory system, one of the functions of the controller is keeping the partial CO_2-pressure in arterial blood at a nominal level. When this pressure is viewed as the input of the controller, it is easy to see that the amount of information in this input decreases because of the controller.

An advantage of using rebreathing is that it 'opens the feedback loop' [9]. During rebreathing, the P_{CO2} in the blood linearly rises because of metabolic production and the fact that the subject inhales its own exhaled gases. This of course produces a rise in ventilation, since the body wants to washout the excess of CO_2. Because of rebreathing however, the increased ventilation does not reverse the rise in P_{CO2}, as is the case in the closed loop situation. So, in rebreathing experiments, one essentially observes the system as if functioning in open loop.

Another advantage of rebreathing is that one requires only a simple setup for the experiments. Effectively, only a suitable bag is needed (of course in addition to suitable sensors and a measuring setup). For the creation of a PRB input on the other hand, an elaborate setup is needed, involving such things as computer controlled valves.

Dependencies

By looking at the controller equations, it becomes clear that certain dependencies between parameters exist. Assuming that the total drive is larger than the chemoreflex drive threshold T_D, but smaller than the patterning threshold T_P, the for approach B relevant equations for tidal volume and frequency are:

$$V_T = S1V(D - T_D) + V_b = S1V(SD_c(P_{CO2} - T_c) - T_D) + V_b$$
$$f = S1F(D - T_D) + f_b = S1F(SD_c(P_{CO2} - T_c) - T_D) + f_b$$

Taking P_{CO2} as the input, these equations can be rewritten as:

$$V_T = a_1 \cdot P_{CO2} + b_1$$
$$f = a_2 \cdot P_{CO2} + b_2$$

Assume that values of the four unknown parameters in these equations (a_1, b_1, a_2, b_2) follow from the aforementioned estimation method. By definition, these four are combinations of the seven controller parameters:

$$a_1 = S1V \cdot SD_c$$
$$b_1 = -S1V(SD_c \cdot T_c + T_D) + V_b$$
$$a_2 = S1F \cdot SD_c$$
$$b_2 = -S1F(SD_c \cdot T_c + T_D) + f_b$$

From the seven controller parameters, only V_b and f_b are directly measurable, the rest are unknown. It can easily be seen that when knowing a_1, b_1, a_2 and b_2, not all of the five unknown parameters can be uniquely derived. In fact, it can be shown that for this model structure a maximum of three parameters can be uniquely estimated. Since we want a_1 and a_2 to be independent (no fixed relation between the slopes for tidal volume and frequency), it is assumed that SD_c is known so that S1V and S1F can be estimated. From b_1 and b_2 either T_c or T_D can be estimated. The choice is more or less arbitrary, but we choose T_D.

The problem of dependency of course also arises for approach A. Here, we have only one equation, which contains five parameters:

$$Vdot = S1Vdot \cdot (D - T_D) + Vdot_b$$
$$= S1Vdot \cdot (SD_c(P_{mCO2} - Tc) - T_D) + Vdot_b$$

Just as with approach B, these equations can be rewritten:

$$Vdot = a_3 \cdot P_{mCO2} + b_3$$

The parameters a_3 and b_3 are combinations of the five parameters:

$$a_3 = S1Vdot \cdot SD_C$$
$$b_3 = -S1Vdot(SD_C \cdot T_c + T_D) + Vdot_b$$

Again, only the basal value $Vdot_b$ is measurable, so that four parameters remain for estimation. Theoretically, when knowing only a_3 and b_3, two parameters can be estimated. The choice for either S1Vdot or SD_c is arbitrary, since the equation only contains the multiplication of S1Vdot and SD_c. We choose S1V, which means that SD_c is assumed nominal. For the second parameter we choose T_D, just like in approach B. Thus, for approach A we define S1Vdot and T_D as the parameters to be estimated.

Next, the cost functions for the two approaches have to be chosen. For approach A, the cost function is simply taken as the sum of the squared errors between measured data and model output:

$$J = \sum (Vdot_d - Vdot_m)^2$$

In this function the subscript *d* denotes the measured data and *m* the model output.

Since in approach B we want to fit two model outputs simultaneously, the choice of a cost function is less trivial than in the case of just one output. Minimization of the following cost function puts an equal weight on both frequency and volume and gives a good fit of both:

$$J = \sum \left[(V_m(f_d - f_m))^2 + (f_m(V_d - V_m))^2 \right]$$

Again, subscript *d* denotes the measured data and *m* the model output.

Providing that a good enough fit is possible, it is expected that the second approach produces estimates with the least uncertainty, since more data – and thus more information – is available.

Parameter Reliability

If performed correctly on a sufficiently rich dataset, the estimation procedure leads to numerical values for the parameters S1V, S1F and T_D. An important question is: how accurate are these values? The reliability of the estimated parameters is investigated by using the Monte Carlo Parameter Sets approach, as described by Lutchen et al [11]. This approach gives an approximation of the 100(1-α)% joint confidence region of the parameters from a single dataset/measurement, by evaluating how much the parameters can vary from

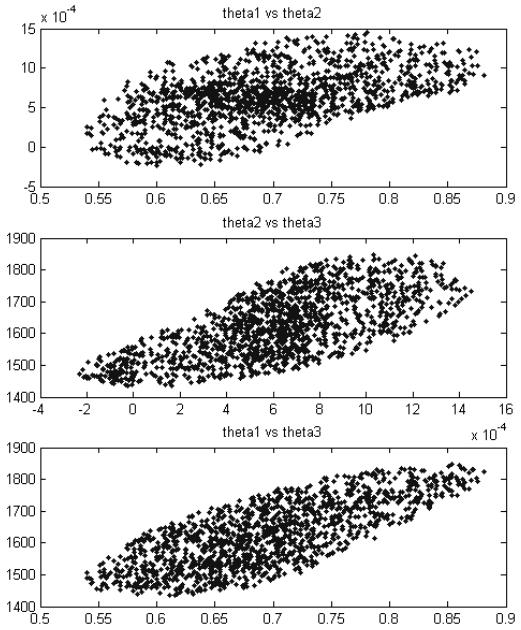

Fig. 4. Example of a non-ellipsoid three-parameter confidence region.

their optimised values such that the resulting increase in the cost function is statistically indistinguishable from the minimized cost function. In other words, we want to find the values of the parameter vector θ for which the following holds:

$$\Delta J = J(\theta) - J(\theta^*) < \varepsilon$$

Where θ^* is the optimised parameter vector and ε is the error bound [12]:

$$\varepsilon = p \cdot \sigma^2 \cdot F_{1-\alpha}(p, n-p)$$

In this equation p is the number of parameters, n is the number of samples, σ^2 is the noise variance and F(a,b) is the F-distribution for (a,b) degrees of freedom. Under the assumption that the model structure is correct and contains no unmodeled dynamics, the noise variance can be approximated as [11]:

$$\sigma^2 = \frac{J(\theta^*)}{n-p}$$

With this method, one can approximate the joint confidence region of each dataset. In the linear case, these have the shape of a p-dimensional ellipsoid, but non-linearities may change the shape of the region (as can be seen in figure 4). How must this confidence region be interpreted? Well, assume that we have computed the 95% confidence region for an estimated parameter combination

from a certain dataset. This can also be done for other datasets, which will produce somewhat different estimations and regions. The '95%' means that for 100 computed intervals, the true value of the parameters is contained in 95 of these intervals [1].

Measurements

Data for the estimation procedure is acquired by performing several rebreathing experiments on different test subjects.

Measuring Protocol

The data presented in this study is based on the respiratory response of two test subjects, both healthy, non-smoking men around the age of 25.

The experimental setup used in the measurements consists of a 12 litre rebreathing bag, which is connected to a mouthpiece. Since we want to measure in the situation of hyperoxia, it is necessary that the bag is filled with oxygen at the start of rebreathing. For the filling of the bag with 100% O_2 (medical gas, provided by Hoek en Loos), the bag can be easily disconnected from the mouthpiece. Connected to the mouthpiece are a capnograph (Weinmann Capnosleep), with a resolution of ±2 mmHg between 3 and 38 mmHg and ±5% between 39 and 75 mmHg, and a spirometer (Cosmed Microquark) with an accuracy of ±2%. By means of a built in temperature sensor, the spirometer automatically converts the measured Ambient Temperature Pressure Saturated (ATPS) units to Body Temperature Pressure Saturated (BTPS) units for use in the model. The capnogram is measured continuously and sampled with a period of 0.05 seconds, while the volume flow can only be measured for five periods of 50 seconds, separated by a short variable time (several seconds). The sample time of the spirometer data is 0.01 seconds.

During a rebreathing test the following steps are performed:

1. At the start of the test, the subject breathes room air through the mouthpiece until ventilation is stable. The measurements are continued for several minutes, in order to acquire data for determination of the basal values.
2. During this time, the detached rebreathing bag is emptied, and then filled with 100% O_2. It is not essential that the bag contains exactly 100% oxygen; a small amount of mixture with room air is allowed.
3. Next, the rebreathing bag is connected to the mouthpiece, and the subject starts rebreathing. A nose clip is worn by the subject to prevent loss of volume.
4. Rebreathing is continued until P_{ETCO2} equals 60mmHg (measured by the capnograph). The experiment is also stopped when the test subject feels uncomfortable. During each 50s period, the subject is asked to hold his breath for several seconds. This allows for synchronisation between data from spirometer and capnograph (as will be discussed later).
5. Resting periods of at least 45 minutes separate repeated tests on the same subject, and no more than three rebreathing tests per day are performed on each subject.

Results

As stated before, the chosen controller parameters are estimated by fitting the model output to the measured data. The processing of the data is done on a PC with Mathworks' Matlab. First, the volume and capnograph data are synchronised by using the short periods of breath holding as described in step 4 of the experiment. Synchronisation is possible since breath holding is visible in both volume and capnograph data as a prolonged constand period. After synchronisation, the relevant values (i.e. maxima and minima of the volumedata and end-expiratory and end-inspiratory values for the capnograph-data) are selected from the data. From this selection the frequency, tidal volume and total ventilation can be computed. Since the end-tidal partial CO_2-pressure, the pressure at the end of expiration, equals the pressure in the alveoli at the end of the previous inspiration, the timestamps of the end-inspiratory values are synchronised with the respective timestamps of the end-tidal CO_2-pressures. This is illustrated in figure 5.

After the data processing, Matlab is used for the

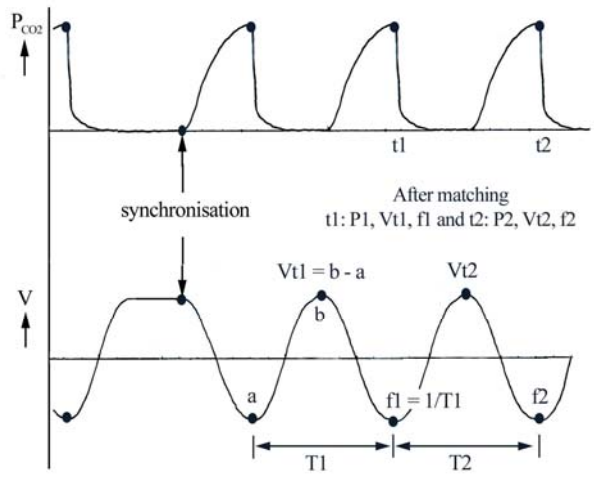

Fig. 5. Processing data by synchronisation and matching the timestamps.

Subject A, approach A

Data (n)	S1Vdot (10^{-2})	TD (10^{3})	$Vdot_b$	$\varepsilon / J(\theta^*)$ (%)
1 (22)	1.24 ± 0.104 (8%)	2.11 ± 0.055 (3%)	9.5	35.3
2 (22)	0.63 ± 0.142 (22%)	1.75 ± 0.146 (8%)	10.1	34.6
3 (26)	1.17 ± 0.111 (10%)	1.70 ± 0.067 (4%)	10.6	28.2
4 (23)	1.47 ± 0.095 (7%)	1.70 ± 0.045 (3%)	11.4	32.6
5 (30)	2.07 ± 0.141 (7%)	1.91 ± 0.044 (2%)	10.6	23.6
6 (26)	1.78 ± 0.086 (5%)	1.78 ± 0.033 (2%)	11.8	28.2
All (# = 6)	1.39 ± 0.504 (36%)	1.82 ± 0.160 (9%)		

Subject A, approach B

Data (n)	S1V	S1F (10^{-3})	TD (10^{3})	fb	Vb	$\varepsilon / J(\theta^*)$ (%)
1 (44)	0.74 ± 0.091 (12%)	2.89 ± 0.41 (14%)	2.00 ± 0.092 (5%)	8.4	1.1	21.8
2 (44)	0.67 ± 0.074 (11%)	0.60 ± 0.35 (58%)	1.59 ± 0.100 (6%)	8.5	1.0	21.9
3 (52)	1.09 ± 0.098 (9%)	0.24 ± 0.33 (138%)	1.57 ± 0.076 (5%)	9.5	1.0	18.4
4 (46)	0.96 ± 0.041 (4%)	1.24 ± 0.24 (19%)	1.19 ± 0.043 (4%)	8.9	0.8	20.4
5 (60)	1.16 ± 0.066 (6%)	3.60 ± 0.26 (7%)	1.81 ± 0.039 (2%)	9.7	1.0	15.4
6 (52)	1.17 ± 0.049 (4%)	2.42 ± 0.16 (6%)	1.74 ± 0.031 (2%)	9.9	1.2	17.1
All (# = 6)	0.97 ± 0.216 (22%)	1.83 ± 1.34 (73%)	1.65 ± 0.275 (17%)			

Table 1. Results of the parameter estimation procedure for subject A for the two described approaches. In approach A, the total ventilation is fit to the model output, while in approach B, frequency and tidal volume are fit simultaneously. The values are reported as mean ± standard deviation (and percentage of mean), the bottom row in each table gives the mean and standard deviation of the n datasets.

estimation procedure. For the minimisation, the Matlab-function 'fminsearch' is used (with all tolerances on the default setting), which tries to find a minimum in a user-specified cost function by changing certain parameters (also user-specified). In this case, the function to be minimized is the cost function J, whose value depends on the output of the Simulink-model for the evaluated parameter values.

The estimation procedure produces optimal values for the parameters, i.e. the values for which the cost function is minimal, which are the values that produce the best fit of model output to measured data. Next, an approximation of the 95% confidence interval of the estimations is determined by using the Monte Carlo Parameter Sets approach described earlier.

Previously, we have postulated two different approaches, in which certain controller parameters are estimated by fitting either the measured total ventilation (approach A) or the measured tidal volume and frequency to the controller output (approach B), using the measured end-tidal P_{CO2} as the input of the model. The basal values of total ventilation, frequency and tidal volume, which differ between subjects, are determined from the resting data (step 1 in the experimental protocol).

Using the two approaches with the experimental data produces the results as shown in Table 1 and 2. To get an idea of the allowed deviation of the cost function J in the MCPS-approximation of the confidence regions, the ratio between ε and the optimal value for J is also shown.

Discussion

The goal of this investigation was to implement a model of the human respiratory system and use this model for parameter estimation, by fitting measured data to the model output.

The gas-exchange part ('plant') of the implemented model is an adaptation of the description by Chiari et al [2]. This model includes the blood shunt, which has a nominal value of 2.4%. One could argue that modelling the shunt is unnecessary, since its value is very small. For partial pressures in the normal working range, this argument is correct. For larger pressures however, the shunt cannot be neglected. Assume for example that the partial oxygen pressure in the alveoli equals 175 mmHg, which corresponds to a saturation of 99% or a concentration of 195 ml O_2 per litre blood (following from the reference dissociation curve). The O_2 concentration in the veins is assumed to be 145 ml/l. Neglecting the shunt, upon passing the lungs the blood will be replenished with oxygen up until a saturation of 99% (195 ml/l). However, with a shunt of 2.4% (nominal value), the amount of arterial oxygen equals:

$$C = (1-s)\cdot C_e + s\cdot C_v$$
$$= 0.976\cdot 195 + 0.024\cdot 145 = 193.8 ml/l$$

This seems a small difference compared to the 195 ml/l in the case of no shunt, but a conversion of

Subject B, approach A

Data (n)	S1Vdot (10^{-2})	TD (10^{3})	$Vdot_b$	$\varepsilon / J(\theta^*)$ (%)
1 (66)	2.02 ± 0.093 (5%)	1.71 ± 0.025 (2%)	13.6	9.9
2 (68)	2.35 ± 0.060 (3%)	1.47 ± 0.014 (1%)	15.3	9.6
3 (44)	2.15 ± 0.119 (6%)	1.68 ± 0.022 (1%)	16.6	15.3
4 (38)	1.78 ± 0.171 (10%)	1.69 ± 0.059 (4%)	18.0	18.0
5 (48)	1.48 ± 0.147 (10%)	1.55 ± 0.047 (3%)	21.5	13.8
All (# = 5)	1.95 ± 0.337 (17%)	1.62 ± 0.105 (6%)		

Subject B, approach B

Data (n)	S1V	S1F (10^{-3})	TD (10^{3})	fb	Vb	$\varepsilon / J(\theta^*)$ (%)
1 (132)	0.65 ± 0.027 (4%)	5.50 ± 0.34 (6%)	1.66 ± 0.025 (2%)	19.8	0.7	6.5
2 (136)	0.80 ± 0.035 (4%)	2.52 ± 0.39 (15%)	1.52 ± 0.024 (2%)	25.6	0.6	6.1
3 (88)	0.68 ± 0.075 (11%)	6.52 ± 0.86 (13%)	1.63 ± 0.050 (3%)	15.8	1.0	9.5
4 (76)	0.61 ± 0.086 (14%)	3.93 ± 0.61 (16%)	1.51 ± 0.100 (7%)	11.8	1.4	11.9
5 (96)	0.46 ± 0.056 (12%)	3.89 ± 0.58 (15%)	1.50 ± 0.061 (4%)	15.2	1.4	8.7
All (# = 5)	0.64 ± 0.123 (19.2%)	4.47 ± 1.56 (35%)	1.56 ± 0.075 (5%)			

Table 2. Results of the parameter estimation procedure for subject B for the two described approaches. In approach A, the total ventilation is fit to the model output, while in approach B, frequency and tidal volume are fit simultaneously. The values are reported as mean ± standard deviation (and percentage of mean), the bottom row in each table gives the mean and standard deviation of the n datasets.

193.8ml/l to partial pressure leads to a value of 130mmHg. This differs significantly from aforementioned 175mmHg, which of course is a direct effect of the flatness of the O_2 dissociation curve for high partial pressures. The effect of the shunt decreases as the partial oxygen pressure gets smaller, because the dissociation curve is far less flat there.

For the implementation of the oxygen dissociation curve a lookup-table containing reference data is chosen, instead of the usual approach of deriving a mathematical formula that fits the reference data. This guarantees accuracy, under the assumptions made (e.g. no influence of temperature and 2,3-DPG). It must be noted that the contribution of the O_2 solved in the blood plasma with regard to the total amount of oxygen in the blood is neglected. When the partial oxygen pressure is at nominal level this does not introduce large errors, since then the amount of solved O_2 is very small. However, for large P_{O2}s, as in the described hyperoxic rebreathing experiments, larger quantities of oxygen are dissolved. A possible improvement of the model is accounting for the solving of oxygen in the plasma, which is not a trivial adaptation.

For the CO_2 dissociation curve, a linear approximation of the 'real' curve is used. Since no numerical reference values for the CO_2-curve were found in literature, the exact error introduced by the linearisation could not be studied. An advantage of the availability of a numerical reference curve is the possibility of using a lookup-table in the model instead of a mathematical description, as is done for the O_2-curve. It can be expected that this will improve the accuracy of the CO_2 curve. Using a lookup-table or an accurate, non-linear mathematical expression will also solve the problem that during the performed rebreathing experiments, the partial CO_2 pressure increases beyond the normal working range, where the accuracy of the linear approximation decreases.

The controller used in the model is the one described by Duffin et al [3]. This relatively simple controller is more or less a variable gain (with some non-linearities, such as saturations), dependent of the partial CO_2 and O_2 pressures in blood and brain. The controller contains no dynamics, which is one of the main reasons why in this case a PRB-testsignal, which has rich frequency content, is not expected to result in far better data for controller estimation. Fitting the data, as will be described further on, proves that this model produces a fairly accurate description of the responses measured in hyperoxic rebreathing experiments, under the condition that the Vdot output of the controller is used. It can however not be concluded that this combination of plant and controller is equally suitable for different kinds of experiments. For example, phenomena like hypoxic ventilatory depression [19], periodic breathing or sleep apnea [7] most likely cannot be explained or simulated by using this model. Another, more elaborate (dynamical) model of the chemoreceptor response may be needed for this. Also, in this study only the situation of hyperoxia is evaluated, there is no verification that the model is correct for other situations, e.g. hypoxia.

Since the presented model, like all models, is merely a simplified description of the real respiratory system, it is inevitable that several

assumptions will have to be made, with regard to both the plant and controller. These are mentioned in Appendix A. Some of the assumptions mentioned are clearly not true when performing the experiments. For example, during rebreathing the respiration increases significantly, which can be compared to light exercise. As such, the assumption that the subject is in rest does not hold.

After implementation of the model in Simulink, the model is used for the estimation of controller parameters. It is assumed that the peripheral chemoreflex is suppressed (which is true in a situation of hyperoxia), because this lowers the amount of parameters to be estimated. Identifying the controller while both peripheral and central reflexes are active is much more difficult. The parameters to be estimated were chosen by looking at the structure of the controller, and by studying the existing dependencies of the controller equations.

In order to acquire data for estimation of the central parameters, two subjects took part in a set of hyperoxic rebreathing experiments, during which they inhaled (part of) their own exhaled gases from a 12 litre bag, starting with a bag filled with 100% oxygen (to create hyperoxia). The main problem with these experiments, which is the problem in all kinds of respiratory experiments with awake, alert subjects, is that it is difficult to recreate natural, spontaneous breathing in a laboratory setting. For example, in our case the subject has to breathe through a mouthpiece while wearing a nose clip, which hardly represents a natural situation. It is easy to see that this will have an influence on the (pattern of) respiration. Furthermore, during the experiment, it is possible for the subject to (un)willingly influence the pattern of breathing, for example when focusing too much on the breathing. One measure that can help to prevent this, is to divert the attention of the subject. In the described experiments this is done by playing music. However, it is necessary for the subject to be alert because of the requests for breath holding. This is one of the reasons why it cannot be guaranteed that the influence of the subjects own will is entirely absent.

During the experiments, the in- and exhaled CO_2 is measured and recorded, as well as the volume flow through the mouthpiece (from which tidal volume and frequency can be derived). The inspired partial O_2-pressure is used in the model, but is not measured during the experiments. As such, certain assumptions must be made for the oxygen pressures. In this case we assume that during the course of each experiment, the inspired partial pressure is large enough to suppress the peripheral chemoreceptor. A small calculation shows the validity of this assumption. At the start of the experiment, the rebreathing bag contains roughly 12 litres of oxygen. Assuming an average oxygen consumption of 0.2 litres per minute and an experiment duration of five minutes, 1 litre O_2 is consumed during the experiment. This leaves 11 litres of oxygen in the bag, which is more than enough to create a situation of hyperoxia.

For the sampling of the volume- and CO_2-data, sample frequencies of 100Hz and 20Hz are used respectively. Because of the low frequency nature of the human respiration (nominally around 0.25Hz) and the fact that in this study only a small portion of the acquired data is used, these sample frequencies are much too high. Assuming a hypothetical upper limit on the breathing frequency of 100 breaths per minute, the highest frequency in the signal equals $100/60 \approx 1.7$Hz. Theoretically (Nyquist), a sample frequency of $2*1.7\text{Hz} = 3.4$Hz would be enough. However, sampling with a higher frequency does not introduce large disadvantages, other than the fact that it produces larger data-files, and thus requires more storage capacity.

The experimental setup used in this study has some limitations. The main restriction is that the spirometer can only measure a maximum of five periods of 50s, separated by short pauses of several seconds. The variable length of these pauses introduces the need for some sort of synchronisation between capnograph and spirometer data. As stated in the experiment description, this synchronisation is performed by using the short periods of breath holding, which take place once in each 50s segment. It can be shown that a few seconds of breath holding only has an effect on respiration for one breath cycle. This means that by removing the breath holding from the data together with the following cycle, the resulting data can be treated as if no breath holding took place.

After processing, the measured data is used for the estimation of certain controller parameters. This is realised by taking the measured end-tidal P_{CO2}, which is assumed to be equal to the capillary pressure, and fit the model output to the measured ventilatory data by tuning the parameters. By using the end-tidal P_{CO2} as an input for estimation, it is implied the brain compartment (where the conversion of arterial CO_2-pressure to medullar pressure takes place) is correctly described. Of course, it would be preferred to also estimate the brain compartment, but this is impossible due to experimental limitations.

To investigate the reliability of the estimations, the Monte Carlo Parameter Sets (MPCS) approach as

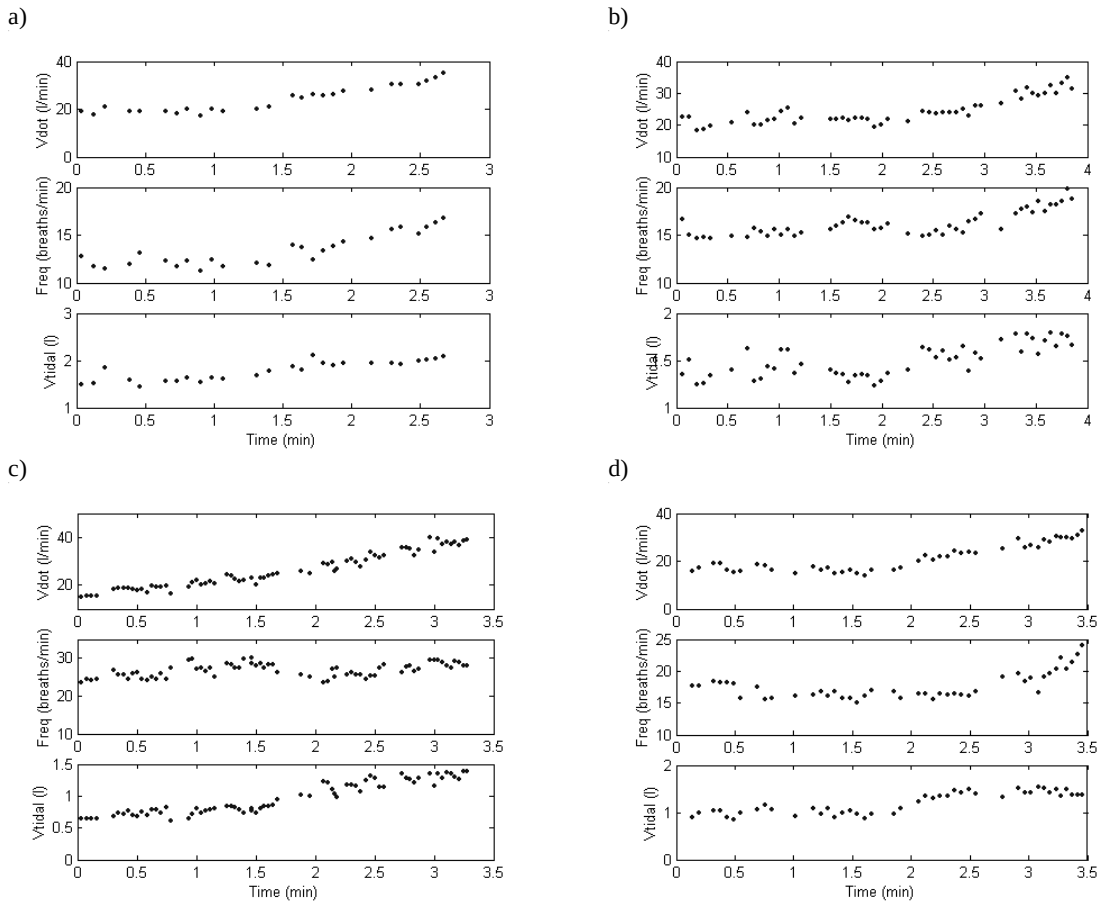

Fig. 6. Intra-subject variation in breathing pattern for several identically setup hyperoxic rebreathing tests: 6a) linear rise in both frequency and tidal volume, 6b) linear rise in frequency, quasi-erratic course of tidal volume 6c) linear rise in tidal volume, quasi-erratic course of frequency, 6d) other possible form

described by Lutchen et al [12] is used. This gives a good indication of the uncertainty of the estimations when the parameters under investigation are allowed to change simultaneously. One of the main advantages of this approach is that it takes non-linearities into account. But there are also limitations to the method. The main limitation is that this method assumes that the model is correct, which implies that there are no unmodeled dynamics. Of course, this is never the case: there will always be a difference between model fits and data (i.e. a non-random distribution of residuals). This increases σ^2, which leads to an overestimation of the parameter uncertainty bounds. Furthermore, when the discrepancy between model output and data is too large (i.e. a 'bad fit'), as is sometimes the case in approach B (e.g. subject A, set 3), the expressed confidence regions lose most of their relevance. Thus, the resulting variances in the parameter estimations as presented in this paper can only be treated as rough approximations.

In examining the results of the estimation procedure and the MCPS confidence region approximation, one of the conclusions is that parameter T_D (chemoreflex threshold) can be estimated with low uncertainty and relatively small variation in the estimates. Another remarkable observation is that the breathing patterns of the subjects seem to vary per experiment (figure 6). In some tests, both frequency and tidal volume show the expected linear rise, while in some tests only tidal volume shows a clear rise and the frequency more or less fluctuates around a constant value (and vice versa), and several other forms were also observed. In some cases this leads to a bad fit of frequency and/or tidal volume, since approach B assumes that both tidal volume and frequency show a linear course. In the estimation results, the uncertainty of the estimated parameters gives an indication of the allowed deviation and thus of the quality of fit. For example, it can be seen that for parameter S1F, which is the slope for the breathing frequency, fairly large uncertainties in the estimations exist, sometimes indicating an almost erratic course of frequency (figure 7). The cause for the variation in breathing pattern is not clear (although it has been shown that each human has a unique pattern, this pattern is reproducible under identical circumstances [18]), but it is not unlikely

that the varying pattern is (at least partly) caused by the laboratory setting and the awareness of the subject, as discussed before. Nevertheless, even though a variation in frequency and tidal volume response exist, fitting the total the total ventilation (approach A) gives estimations with relatively low uncertainty in most cases. This is logical: the total ventilation has to rise because of the increasing CO_2 in the body, regardless of the way in which this is accomplished. In other words, the product of tidal volume and frequency has to rise in a specific way (in this case linear) to satisfy the desire of the body to washout more CO_2. Taking this into account, approach A is the preferred approach. This also means that when designing a general model for the respiratory controller (one that is applicable for the 'average person'), as is done by Duffin et al [3], it makes more sense to base this on the total ventilation, than to separately model the frequency and tidal volume.

Conclusions

The human respiration is a system that normally operates in closed loop and contains several non-linearities. In this study a model of the respiratory system is presented, based on models found in literature, and an attempt was made to identify the respiratory controller in hyperoxia. As a part of the modelling of the gas exchange in lungs and tissue a fairly novel approach is taken in implementing the oxygen dissociation curve, namely the use of a lookup-table with reference values instead of a mathematical approximation. The resulting model, implemented in Simulink, can be used to simulate the respiratory response to situations like hypoxia, hypocapnia, hyperoxia or asphyxia. In this study, the focus is on the response to hyperoxic rebreathing. One of the goals of this study was to estimate the parameters of the controller model, by fitting model output(s) to measured data. However, due to several dependencies between parameters for the implemented controller, the amount of parameters that can be uniquely estimated is limited. Data for the estimation is acquired by performing rebreathing experiments, which circumvents some of the problems associated with closed loop identification (such as decrease of information because of feedback). Two subjects took part in several rebeathing tests, all performed in hyperoxia, which suppresses the peripheral chemoreflex. In order to study the reliability of the estimations, the joint confidence region of the estimation is acquired by using a Monte Carlo approach. The big advantage to this (little used) method is that is specifically takes non-linearities into account. It is important to note that this method only produces an approximation of the confidence regions. Nevertheless, as follows from the estimation results, this approximation gives a good indication of the uncertainty of the estimation and the quality of fit. Of the two approaches to parameter estimation that are described, the first one, which takes the total ventilation output of the controller and fits this to the measured ventilation, produces estimates of the parameters S1Vdot and T_D with only moderate uncertainty. The second approach, whereby both the frequency and tidal volume outputs are fit to measured data by tuning the slopes S1F and S1V, as well as T_D, produces larger uncertainties for the slopes. Furthermore, for the performed rebreathing tests significant variations between the tidal volume and breathing frequency responses were observed within both subjects, indicating a strong variation in breathing pattern per experiment. It is not unlikely that this intra-subject variation in pattern is – at least partly – caused by the awareness of the subject, the laboratory-setting (which may lead to mild forms of anxiety in the subject) and the unnatural means of breathing (e.g. while wearing a noseclip, and breathing through a tube). Because of the variations, it is sometimes impossible to get a good linear fit of frequency or tidal volume. In almost all of these cases however, a fit of total ventilation (the first approach) does give proper results with little uncertainty. This suggests that it is more useful to base a general respiratory controller on total ventilation than on tidal volume and frequency.

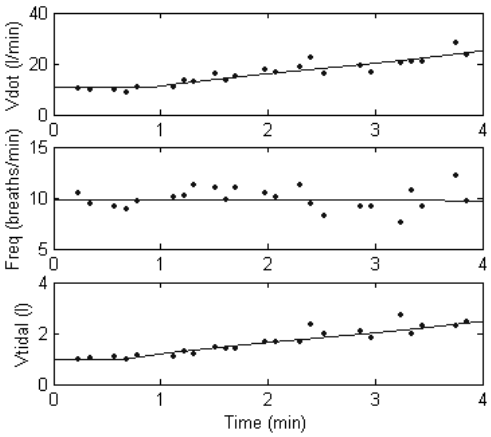

Fig. 6. Dataset with 'erratic' frequency data, including the resulting fits.

Appendix A. Model Assumptions

For the model of the plant, the following assumptions are made:

- The model is based on healthy persons during a state of rest. This means that the metabolism M, heart rate Q and oxygen uptake θ are assumed constant.

- The O_2 consumption is constant and the respiratory quotient RQ (the fraction CO_2/O_2) equals 0.8 for the tissue compartment and 1.0 for the brain compartment.
- The brain blood flow is a constant fraction of the total blood flow.
- The end-tidal partial gas pressure is equal to the partial pressure in the alveoli, which equals the end-capillary pressure.
- Continuous, unidirectional gas flow.
- In the O_2 dissociation curve, the effects of pH, temperature and concentration of 2,3-DPG are neglected.
- In the CO_2 dissociation curve, the effect of temperature is neglected.

The assumptions for the respiratory controller are as follows:

- The respiratory controller has only influence on the circulation, which means that the cardiac output is constant.
- Respiration is determined by three drives: peripheral, central and basal drives.
- The peripheral drive is linearly related to the arterial CO_2-pressure P_{aCO2} with a slope that varies hyperbolically with P_{aO2}. A rise of P_{aO2} results in a decrease in slope.
- A slope constant and a P_{O2} asymptote describe the hyperbolic relation between P_{O2} and P_{CO2}.
- The central drive is linearly related to the CO_2 pressure in the medulla (P_{mCO2}) with a slope that is independent of P_{aO2}.
- The basal drive is independent of both P_{O2} and P_{CO2}.
- The central and peripheral drives share a common chemoreceptor threshold (T_c) and add to produce the total drive.
- The total drive does not affect breathing until a chemoreflex drive threshold (T_D) is exceeded.
- The total drive produces changes in tidal volume, breathing frequency and ventilation that are scaled versions of the drive.
- The pattern of breathing changes when the drive exceeds the patterning threshold (T_P). Below T_P, the rise in total ventilation is mainly caused by an increase in tidal volume while above T_P, the rise in ventilation is caused by an increase in breathing frequency.
- In hyperoxia, the peripheral chemoreflex is completely suppressed.

Appendix B. Nominal Parameter Values [2], [3] and Steady State Values of the Model

Parameter	Value	Unit
V_A	3.28	l (BTPS)
V_B	0.90	l (BTPS)
V_T	38.74	l (BTPS)
V_D	0.150	l (BTPS)
λ	863	mmHg
Q	5	l/min
s	0.24	-
z	0.87	-
θ	0.05	l/l
τ_B	5.33	min
k_{cr}	1.139	$min^{1/2}l^{1/2}$
C_{eO2}	0.193	l/l
C_{eCO2}	0.573	l/l
C_{aO2}	0.192	l/l
C_{aCO2}	0.574	l/l
C_{vO2}	0.142	l/l
C_{vCO2}	0.616	l/l
C_{BO2}	1.01e-3	l/l
C_{BCO2}	0.649	l/l
C_{TO2}	13.0e-4	l/l
C_{TCO2}	0.611	l/l
C_{vBO2}	0.117	l/l
C_{vTO2}	0.145	l/l
P_{IO2}	157	mmHg
P_{ICO2}	0.3	mmHg
P_{AO2}	111	mmHg
P_{ACO2}	39.4	mmHg
P_{mO2}	44.65	mmHg
SD_c	0.132	l/mmHg
T_c	34.1	mmHg
K	1.39	l/mmHg
AP_{O2}	30	mmHg
S1V	1	-
S1F	0.00518	breaths/min/l
S1Vdot	0.024	min^{-1}
S2V	0.338	-
S2F	0.0105	breaths/min/l
S2Vdot	0.0367	min^{-1}
T_P	2879	ml
T_D	1539	ml
$Vdot_b$	6.38	l/min
$Vdot_D$	1.74	l/min
V_b	550	ml
f_b	11.6	breaths/min

References

1. Bard, Y. *Nonlinear Parameter Estimation*, p. 186, Academic Press, New York, 1974.
2. Chiari, L., G. Avanzolini and M. Ursino. *A Comprehensive Simulator of the Human Respiratory System - Validation with Experimental and Simulated Data*, Ann Biomed Eng, Vol. 25, No. 6, 1997, p. 985-999.
3. Duffin, J., R.M. Mohan, P. Vasilou, R. Stephenson and S. Mahamed. *A model of the chemoreflex control of breathing in humans: model parameters measurement*, Respir Physiol, No. 120, 2000, p. 13-26.
4. Grodins, F.S., J. Buell and A.J. Bart. *A Mathematical analysis and digital computer*

simulation of the respiratory control system, J Appl Physiol, No. 22, 1967, p. 260-276.
5. Ghazanshahi, S.D and M.C.K. Khoo. *Estimation of Chemoreflex Loop Gain Using Pseudorandom Binary CO_2 Stimulation.* IEEE Trans Biomed Eng, Vol. 44, No. 5, 1997, p. 357-266.
6. Guyton, A.C. and J.E. Hall, *Textbook of Medical Physiology – ninth edition*, W.B. Saunders Company, 1996, Philadelphia.
7. Hudgel, D.W., E.A. Gordon, S. Thanakitcharu and E.N. Bruce, *Instability of Ventilatory Control in Patients with Obstructive Sleep Apnea*, Am J Respir, Vol. 158, 1998, p 1142-1149.
8. Kelman, R.G. *Digital computer subroutine for the conversion of oxygen tension into saturation*, J Appl Physiol, Vol. 21, No. 4, 1966, p. 1375-1376.
9. Khoo, M.C.K. *Physiological Control Systems: analysis, simulation, and estimation*, IEEE Press, New York, 2000.
10. Longobardo, G., C.J. Evangelisti, N.S. Cherniak, *Effects of neural drives on breathing in the awake state in humans*, Respir Physiol, No. 129, 2002, p. 317-333.
11. Lutchen, K.R. and A.C. Jackson. *Confidence Bounds on Respiratory Mechanical Properties Estimated from Transfer Versus Input Impedance in Humans Versus Dogs*, IEEE Trans Biomed Eng, Vol. 39, No. 6, 1992, p. 644-651.
12. Lutchen, K.R. and A.C. Jackson. *Statistical Measures of Parameter Estimates from Models Fit to Respiratory Impedance Data: Emphasis on Joint Variabilities*, IEEE Trans Biomed Eng, Vol. 33, No. 11, 1986, p. 1000-1009.
13. Severinghaus, J.W. *Blood Gas Calculator*, J Appl Physiol, Vol. 21, No. 3, 1966, p. 1108-1116.
14. Severinghaus, J.W. *Simple, accurate equations for human blood O_2 dissociation computations*, J Appl Physiol, Vol. 46, No. 3, 1979, p. 599-602.
15. Sharan, M., M.P. Singh and A. Aminataei. *A mathematical model for the computation of the oxygen dissociation curve in human blood*, Biosystems, No. 22, 1989, p. 249-260.
16. Siggaard-Andersen, O., P.D. Wimberly, I. Göthgen and M. Siggaard-Andersen, *A Mathematical Model of the Hemoglobin-Oxygen Dissociation Curve of Human Blood and of the Oxygen Partial Pressure as a Function of Temperature*, Clin Chem, Vol. 30, No. 10, 1984, p. 1646-1651.
17. Ursino, M. and E. Magosso, *A theoretical analysis of the carotid body chemoreceptor response to O_2 and CO_2 pressure changes*, Respir Physiol, No. 130, 2002, p. 99-110.
18. Benchetrit, G. *Breathing pattern in humans: diversity and individuality*, Respir Physiol, No. 122, 2000, p. 123-129.
19. Powell, F.L. W.K. Milsom and G.S. Mitchell, *Time domains of the hypoxic ventilatory response*, Respir Physiol, No. 112, 1998, p. 123-134.